GEOPHYSICAL RESEARCH LETTERS, VOL. 33, L15821, doi:10.1029/2006GL026162, 2006

Atmospheric constraints on global emissions of methane from plants

S. Houweling,[1,2] T. Röckmann,[2] I. Aben,[1] F. Keppler,[3] M. Krol,[2] J. F. Meirink,[2] E. J. Dlugokencky,[5] and C. Frankenberg[6]

Received 27 February 2006; revised 1 June 2006; accepted 12 June 2006; published 15 August 2006.

[1] We investigate whether a recently proposed large source of CH_4 from vegetation can be reconciled with atmospheric measurements. Atmospheric transport model simulations with and without vegetation emissions are compared with background CH_4, δ^{13}C-CH_4 and satellite measurements. For present–day CH_4 we derive an upper limit to the newly discovered source of 125 Tg CH_4 yr^{-1}. Analysis of preindustrial CH_4, however, points to 85 Tg CH_4 yr^{-1} as a more plausible limit. Model calculations with and without vegetation emissions show strikingly similar results at background surface monitoring sites, indicating that these measurements are rather insensitive to CH_4 from plants. Simulations with 125 Tg CH_4 yr^{-1} vegetation emissions can explain up to 50% of the previously reported unexpectedly high CH_4 column abundances over tropical forests observed by SCIAMACHY. Our results confirm the potential importance of vegetation emissions, and call for further research. **Citation:** Houweling, S., T. Röckmann, I. Aben, F. Keppler, M. Krol, J. F. Meirink, E. J. Dlugokencky, and C. Frankenberg (2006), Atmospheric constraints on global emissions of methane from plants, *Geophys. Res. Lett.*, *33*, L15821, doi:10.1029/2006GL026162.

1. Introduction

[2] One year ago it was thought that the major processes that control atmospheric methane had been identified, and that the main remaining task was to reduce the uncertainties in the source and sink estimates. Recent findings have demonstrated, however, that we have not reached that stage yet. Firstly, *Frankenberg et al.* [2005] presented comparisons of SCIAMACHY CH_4 retrievals and transport model calculations pointing to a missing source over tropical forests. Secondly, *Ferretti et al.* [2005] found a surprising variation of δ^{13}C-CH_4 in Antarctic ice cores prior to the start of industrialization and a plateau from 1000 to 1500 AD that was about 3‰ heavier than expected from commonly accepted preindustrial methane budgets. Third and presumably most importantly, *Keppler et al.* [2006] discovered that methane is emitted by living plants and plant litter under oxic conditions, adding a new source term to the methane budget. From the limited experimental evidence that is currently available it is difficult to derive a reliable global source estimate. Initial attempts by *Keppler et al.* [2006] yield global emissions between 62 and 236 Tg CH_4 yr^{-1}. Even the low end of this range requires re-evaluation of the global CH_4 budget, but, to do this effectively, the range must be narrowed considerably. Interestingly, the isotopic signature and the expected geographical distribution of vegetation emissions help to explain the results of *Frankenberg et al.* [2005] and *Ferretti et al.* [2005].

[3] Uncertainties of methane emissions from vegetation can be reduced by additional closed chamber measurements to characterize the process in further detail, allowing improved source extrapolation. An alternative is to deconvolute information on vegetation emission that is present in atmospheric measurements using inverse modelling techniques [see, e.g., *Bergamaschi et al.*, 2005]. Here we report forward model simulations, as an initial step toward inverse modelling, to explore what atmospheric signals are expected and to search for evidence in existing observations. We investigate the range of vegetation emissions that can be brought into agreement with three sources of observational evidence: 1) preindustrial (1000–1500 AD) and present–day global mean CH_4 and δ^{13}C-CH_4, 2) large–scale concentration variations as observed at remote surface sites, 3) SCIAMACHY CH_4 retrievals. Firstly, global source scenarios are constructed with and without vegetation emissions, which satisfy the present–day level of CH_4 and δ^{13}C-CH_4. These scenarios are extrapolated to preindustrial times and compared to preindustrial levels of CH_4 and δ^{13}C-CH_4 following the approach of *Houweling et al.* [2000a]. A third source scenario is introduced to improve the agreement under preindustrial conditions. The three scenarios are used as input to the atmospheric transport model TM3 [*Heimann*, 1995]. The model results are compared with background measurements of the NOAA global cooperative air sampling network [*Dlugokencky et al.*, 1994], focusing on the latitudinal gradient and the seasonal cycle. Finally, model simulated total column CH_4 is compared with SCIAMACHY CH_4 retrievals to investigate whether vegetation emissions can explain the elevated CH_4 concentrations observed over tropical forests.

2. Source Scenarios

[4] Three emission scenarios are used as input to the model: no vegetation emissions (S1), maximum vegetation emissions (S2), and reduced vegetation emissions (S3) (see Table 1). The emission scenarios have been designed to satisfy the present–day methane budget, characterized by a quasi steady–state at a global mean concentration of ~1780 ppb on the recently adjusted CH_4 standard scale (NOAA04 [*Dlugokencky et al.*, 2005]), and a mean δ^{13}C at

[1]Netherlands Institute for Space Research, Utrecht, Netherlands.
[2]Institute for Marine and Atmospheric Research Utrecht, Utrecht University, Utrecht, Netherlands.
[3]Max Planck Institute for Nuclear Physics, Heidelberg, Germany.
[4]Department of Meteorology and Air Quality, Wageningen University, Wageningen, Netherlands.
[5]Earth System Research Laboratory, Boulder, Colorado, USA.
[6]Institute of Environmental Physics, Heidelberg University, Heidelberg, Germany.

0094-8276/06/2006GL026162$05.00

Table 1. Summary of Global Emission Scenarios

	S1, Tg yr^{-1}	S2, Tg yr^{-1}	S3, Tg yr^{-1}	$\delta^{13}C$, ‰
		Anthropogenic Fluxes		
coal	38	33	38	−35
oil	10	10	10	−40
gas	49	49	49	−40
rice	80	39	60	−63
burning	45	36	40	−21.7[a]
animals	98	95	103	−62
waste	70	58	70	−55/−61[b]
fuel use	5	5	5	−40
		Natural Fluxes		
wetlands	145	90	80	−61
plants	0	125	85	−49.8
termites	20	20	20	−57
ocean	15	15	15	−60
geologic	18	18	18	−40
	S1	S2	S3	
sum CH_4, Tg yr^{-1}	593	593	593	
sum $\delta^{13}C$, ‰	−53.2	−51.9	−51.9	

[a]C3:C4 = 3:1; burning includes biofuel.
[b]Landfills/waste water.

−47‰ with a 0.3‰ disequilibrium [*Lassey et al.*, 2005]. The methane sink has been parameterized as described by *Houweling et al.* [2000b], resulting in a mean atmospheric lifetime of 8.4 yr (including stratospheric oxidation and soil uptake). This requires a global source of 593 Tg CH_4 yr^{-1} to balance the CH_4 concentration at the current level.

[5] Scenario S1 represents a reference scenario that one might have used prior to the discovery of plant emissions. The methane sources and sinks are taken from [*Houweling et al.*, 2000b], except geological emissions, which are composed of hydrocarbon sediments (7 Tg yr^{-1}), mud volcanoes (7 Tg yr^{-1}) and geothermal emissions (4 Tg yr^{-1}) following [*Etiope and Klusman*, 2002]. Furthermore, slight adjustments of the anthropogenic emissions have been introduced to satisfy the global budgets of CH_4 and $\delta^{13}C$-CH_4. Note that the rice emissions have been kept at a rather high level of 80 Tg CH_4 yr^{-1}, despite recent studies that point toward lower emissions (as in S2). Nevertheless, to satisfy the global budget we choose to keep the older estimate.

[6] Scenario S2 represents the maximum vegetation source that can be supported by the present−day methane budget. In the model, vegetation emissions are distributed proportional to leaf area index (LAI) and scaled by pre-calculated monthly−mean NO_2 photolysis rates to account for the light dependence reported by *Keppler et al.* [2006] (see the auxiliary material[1] for details). The global budget provides an important constraint on the size of vegetation emissions, in the sense that any additional emissions should be accompanied by reductions of other sources to satisfy the overall budget. Candidate processes for compensation are those that are either highly uncertain or might have been confused with plant emissions in the past. We choose to compensate vegetation emissions mainly by reducing natural wetlands. Natural wetlands are a highly uncertain source, in part constrained by the global budgets of present−day and preindustrial methane. They are an attractive option, because compensation of vegetation emissions by a reduction of a natural source leaves both the current and the preindustrial budgets unaffected. In S2 we take all anthropogenic emissions from EDGAR FT2000 [*Aardenne et al.*, 2005]. The anthropogenic emissions of *Houweling et al.* [2000b] were systematically higher than EDGAR adding up to 70 Tg CH_4 yr^{-1}, which we now attribute to vegetation. Wetland and vegetation emissions are chosen such that their sum satisfies the global methane budget and their ratio the isotopic budget, increasing the vegetation emissions by another 55 Tg yr^{-1} resulting in a global source of 125 Tg CH_4 yr^{-1} for S2. According to this scenario the Amazon rain forest contributes 23 Tg CH_4 yr^{-1}, well within the range of 4−38 Tg yr^{-1} of a missing upland source reported by *Braga do Carmo et al.* [2006]. To account for underestimated wetland emissions from tropical forests, the wetland emissions from *Walter and Heimann* [2000] have been redistributed such that 30 Tg CH_4 yr^{-1} is emitted from tropical forests in line with *Melack et al.* [2004].

[7] Scenario S3 is a compromise between S1 and S2, and is outlined in section 3.

[8] In principle, $\delta^{13}C$ should discriminate between the isotopically light wetland emissions and distinctively heavier vegetation emissions for the major source adjustments considered here (isotopic characteristics are listed in Table 1). A complication arises, however, because the isotopic fractionation of the OH sink as measured by *Saueressig et al.* [1995] (3.9‰) is substantially less than assumed previously (5.4‰ [*Cantrell et al.*, 1990]). The newer and presumably more accurate fractionation of 3.9‰ has been difficult to reconcile with the tropospheric level of $\delta^{13}C$-CH_4 in the past, and is therefore also not used for our reference source scenario S1. However, a less fractionating sink fits well in a scenario with vegetation emissions allowing a sizeable shift in the relative contribution of wetlands and vegetation, which is used for S2 and S3 as we aim to derive an upper limit to vegetation emissions. Combining the global constraint on the isotopic budget with the assumed fractionation of the sink, we arrive at a global source of −53.2‰ for a 5.4‰ sink (used in S1), or −51.9‰ for a 3.9‰ sink (used in S2 and S3).

3. Test 1: Preindustrial Budget

[9] S1 can well explain the preindustrial methane level of 710 ppb reported by *Etheridge et al.* [1998] (and adjusted to the NOAA04 scale). However, the corresponding $\delta^{13}C$-CH_4 level of −50‰ cannot be reconciled with the −47‰ measured in air retrieved from Antarctic ice, unless large variations in preindustrial biomass burning emissions are assumed as hypothesized by *Ferretti et al.* [2005]. S2 overestimates the preindustrial methane level by ∼150 ppb, but accurately reproduces medieval $\delta^{13}C$-CH_4. Higher OH levels in preindustrial times would improve the preindustrial level of S2 without affecting $\delta^{13}C$-CH_4. However, to bring S2 in agreement with the preindustrial methane level requires that preindustrial OH was 30% higher than today, instead of 7.5% of *Houweling et al.* [2000a], which seems difficult to justify. These results suggest that S2 overestimates natural sources, although no experimental evidence of preindustrial OH exists to draw firm conclusions. To account for this problem, S3 is

[1]Auxiliary materials are available in the HTML. doi:10.1029/2006GL026162.

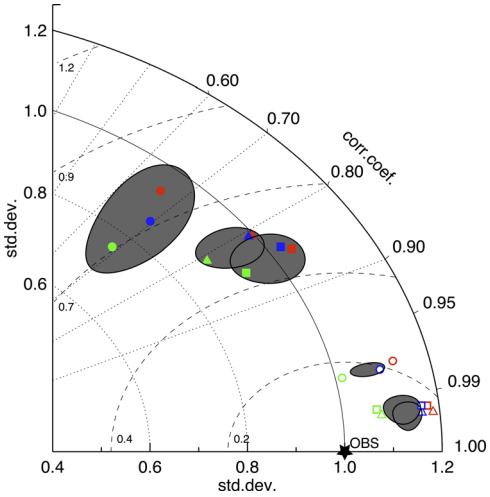

Figure 1. Normalized Taylor plot of model performance for the seasonal cycle (solid symbols) and the latitudinal distribution (open symbols). Circles, full set of stations; triangles, background stations only; squares, same as triangles, but without stations north of 60°N; red, S1; green, S2; blue, S3. Ellipses represent the 95% confidence interval of the combined model and measurement uncertainty.

introduced with a ratio of natural and anthropogenic emissions that reproduces preindustrial and present–day CH_4 and δ^{13}C-CH_4 for a 7.5% change in OH. It implies that a 50 Tg CH_4 yr^{-1} (or 15%) increase of the EDGAR FT2000 anthropogenic emissions is needed to reproduce the CH_4 increase since preindustrial times under our best guess scenario of OH. These emissions are allocated such that a reasonable compromise is obtained between the anthropogenic sources of S1 and S2. Vegetation emissions are reduced from 125 Tg CH_4 yr^{-1} in S2 to 85 Tg CH_4 yr^{-1} in S3.

4. Test 2: Flask Measurements

[10] We analyzed observed and model simulated latitudinal distributions and seasonal cycles of CH_4. TM3 simulations were carried out for each source scenario for the period 2001–2004, initialized with a realistic CH_4 and δ^{13}C-CH_4 global mean and north-south difference. The results are compared with flask measurements that were averaged over the period 1999–2004. Generally, the agreement between model and measurements is quite satisfactory with the model reproducing much of the observed large scale variability. The differences between the scenarios remain surprisingly small despite the sizeable differences in source partitioning (see the auxiliary material for typical examples). The most notable disagreement is found at the higher latitudes of the Northern Hemisphere, where the model simulations underpredict the summer minimum by about 20 ppb. This points to overestimated seasonal variation of the combined emission from wetlands and vegetation, which opposes the predominant seasonal variation caused by OH. Furthermore, the model tends to slightly overpredict the latitudinal gradient (20 ppb for S1), which improves with increasing vegetation emissions (7 ppb for S2).

[11] Figure 1 shows a graphical representation of basic statistical properties introduced by *Taylor* [2001] summarizing the overall performance of our model simulations. It combines the correlation (azimuth angle) and the standard deviations (distance from the origin) of model and measurements, and the RMS difference between them (distance between "OBS" and model symbols). The model performance is tested for different sets of stations indicated by different symbols in Figure 1. Circles refer to all NOAA sites that had at least 3 months of data in each year of the analyzed period. Triangles are similar to circles except that sites are excluded when the interannual variation of a particular month exceeds 17.5 ppb (or ~1%). Squares are similar to triangles, but exclude all sites north of 60°N, to remove the impact of the model overestimated summer concentrations at these sites. Grey ellipses indicate the range of model performance that can be expected given model and measurement uncertainties. More specifically, it represents the 2σ variation of the "performance" of a large number of realizations of randomly perturbed observations. The standard deviation of a single perturbation represents the uncertainty of an observed monthly–mean concentration plus model uncertainty, which is roughly assumed to be half of the observational uncertainty. Since both sources of uncertainty are assumed independent the latter only contributes about 10% to the total. Note that the observational uncertainty mainly represents the interannual variation of the seasonal cycle (the actual measurement error is much smaller).

[12] For the seasonal cycle, the RMS error of the model reduces going from circles to squares. This is expected since the agreement between model and measurement generally improves when moving away from the sources. Simulation S2 slightly underpredicts variability, as indicated by its position left of the solid arc that connects standard deviations of 1 on the X and Y axis. S1 and S3 behave rather similar and under- or overpredict variability dependent on station selection. More importantly, the corresponding grey ellipses encompass the model simulations, indicating that the difference in performance between the simulations S1–S3 is within the uncertainties and therefore not significant. The results for the latitudinal distribution (open symbols) are slightly different. Again, the standard deviation of S2 is smallest, in line with the measurements and explained in part by the reduced north-south gradient. The difference with S1 and S3 exceeds the 2σ interval of the combined model–measurements uncertainty, and therefore the improvement is significant at the 95% confidence level. Apart from this, our model does not show a significant signal of vegetation emissions at the NOAA sites that might confirm or falsify S2.

5. Test 3: SCIAMACHY

[13] The top plot of Figure 2 shows the difference between the SCIAMACHY methane retrievals that were published by *Frankenberg et al.* [2006] and total column methane derived from our model scenario S1. Here we take

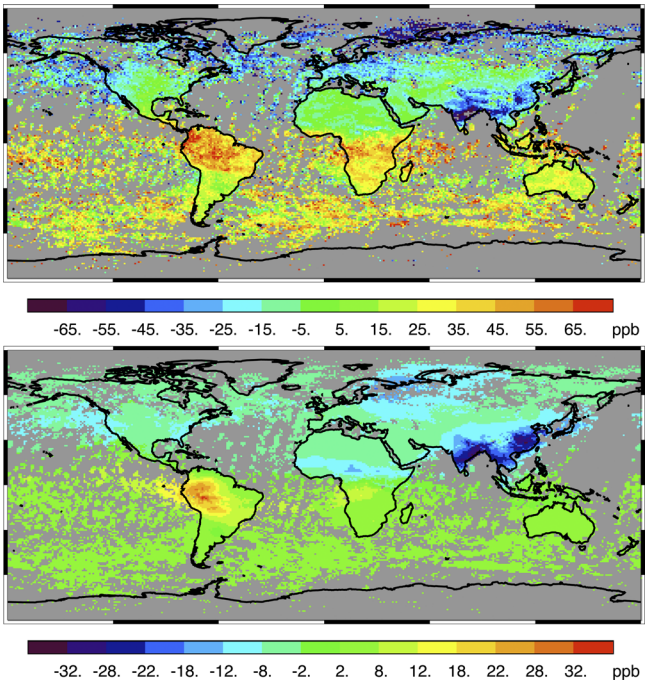

Figure 2. Comparison of SCIAMACHY observed and model simulated total column CH_4 averaged over the period August–November 2003: (top) SCIAMACHY minus S1 and (bottom) S2 minus S1. Note the difference in scale.

into account the vertical averaging kernel of the retrieval and realistic concentration variations of CO_2. Figure 2 confirms the general conclusion by *Frankenberg et al.* [2005], that the model underestimates methane in the tropics. The model overestimates the SCIAMACHY observed north–south gradient, similar to results presented by *Frankenberg et al.* [2005]. S1 overestimates concentrations over South-East Asia, which can be explained by the rather large rice emissions needed to close the global budget. The difference between model and measurements in the tropics is of a similar magnitude as found by *Frankenberg et al.* [2005], although the relation with tropical forests seems less pronounced. The bottom plot in Figure 2 shows the difference between model scenario S2 and S1. If the top and bottom plot of Figure 2 were the same, then S2 would be in perfect agreement with the SCIAMACHY retrievals. It does show similar patterns (note the difference in scale) largely explaining the overestimated emissions over South-East Asia, but accounting for, at most, half of the difference with SCIAMACHY over the Amazon (25% averaged over all tropical forests). Similarly, the modelled north–south gradient changes in the right direction but not enough to explain the measurements.

6. Concluding Remarks

[14] We have made a first assessment of the atmospheric implications of a significant source of methane from vegetation. Most importantly, it seems possible that a large source of methane from vegetation has been overlooked in the past, although it is difficult to explain emissions exceeding 125 Tg CH_4 yr^{-1}. Our analysis of preindustrial methane points to 85 Tg CH_4 yr^{-1} as a more plausible upper bound to vegetation emissions. To derive a best guess estimate on the basis of atmospheric measurements will require inverse modelling. Vegetation emissions do improve the comparison between the model and SCIAMACHY retrievals, although our combined vegetation and redistributed wetland emissions explain only about half of the previously reported discrepancy between model and measurements over the Amazon. It should be realized that we might underestimate the contribution of vegetation emissions from the tropics, given the limited species-specific information that is available at present. On the other hand, the SCIAMACHY CH_4 retrievals over tropical forests require further validation also [see, e.g., *Frankenberg et al.*, 2006]. A multidisciplinary research effort is needed to further characterize and quantify methane emissions from vegetation.

[15] **Acknowledgments.** We thank the SCIAMACHY and ENVISAT teams who have participated in the planning, building, launching and operating of the SCIAMACHY instrument. Further, we thank SARA for the use of their high performance computing facilities.

References

Aardenne, J. A., F. J. Dentener, J. G. J. Olivier, J. A. H. W. Peters, and L. N. Ganzeveld (2005), The EDGAR 3.2 fast track 2000 dataset (32FT2000), technical report, Joint Res. Cent., Ispra, Italy. (Available at http://www.mnp.nl/edgar/model/v32ft2000edgar.)

Bergamaschi, P., M. Krol, F. Dentener, A. Vermeulen, F. Meinhardt, R. Graul, M. Ramonet, W. Peters, and E. J. Dlugokencky (2005), Inverse modelling of national and European CH_4 emissions using the atmospheric zoom model TM5, *Atmos. Chem. Phys.*, *5*, 2431–2460.

Braga do Carmo, J., M. Keller, J. D. Dias, P. B. de Camargo, and P. Crill (2006), A source of methane from upland forests in the Brazilian Amazon, *Geophys. Res. Lett.*, *33*, L04809, doi:10.1029/2005GL025436.

Cantrell, C. A., R. E. Shetter, A. H. McDaniel, J. G. Calvert, J. A. Davidson, D. C. Lowe, S. C. Tyler, R. J. Cicerone, and J. P. Greenberg (1990), Carbon kinetic isotope effect in the oxidation of methane by the hydoxyl radical, *J. Geophys. Res.*, *95*, 22,455–22,462.

Dlugokencky, E. J., L. P. Steele, P. M. Lang, and K. A. Masarie (1994), The growth rate and distribution of atmospheric methane, *J. Geophys. Res.*, *99*, 17,021–17,043.

Dlugokencky, E. J., R. C. Myers, P. M. Lang, K. A. Masarie, A. M. Crotwell, K. W. Thoning, B. D. Hall, J. W. Elkins, and L. P. Steele (2005), Conversion of NOAA atmospheric dry air CH_4 mole fractions to a gravimetrically prepared standard scale, *J. Geophys. Res.*, *110*, D18306, doi:10.1029/2005JD006035.

Etheridge, D. M., L. P. Steele, R. J. Francy, and R. L. Langenfelds (1998), Atmospheric methane between 1000 A. D. and present: Evidence of anthropogenic emissions and climatic variability, *J. Geophys. Res.*, *103*, 15,979–15,993.

Etiope, G., and R. W. Klusman (2002), Geologic emissions of methane to the atmosphere, *Chemosphere*, *49*, 777–789.

Ferretti, D. F., et al. (2005), Unexpected changes to the global methane budget over the past 2000 years, *Science*, *309*, 1714–1717.

Frankenberg, C., J.-F. Meirink, M. van Weele, U. Platt, and T. Wagner (2005), Assessing methane emissions from global space-borne observations, *Science*, *308*, 1010–1014.

Frankenberg, C., J. F. Meirink, P. Bergamaschi, A. P. H. Goede, M. Heimann, S. Körner, U. Platt, M. van Weele, and T. Wagner (2006), Satellite chartography of atmospheric methane from SCIAMACHY on board ENVISAT: Analysis of the years 2003 and 2004, *J. Geophys. Res.*, *111*, D07303, doi:10.1029/2005JD006235.

Heimann, M. (1995), The global atmospheric tracer model TM2, *Tech. Rep. 10*, Dtsch. Klimarechenzent., Hamburg, Germany.

Houweling, S., F. J. Dentener, and J. Lelieveld (2000a), Simulation of preindustrial atmospheric methane to contrain the global source strength of natural wetlands, *J. Geophys. Res.*, *105*, 17,243–17,255.

Houweling, S., F. J. Dentener, J. Lelieveld, B. Walter, and E. J. Dlugokencky (2000b), The modeling of tropospheric methane: How well can point measurements be reproduced by a global model?, *J. Geophys. Res.*, *105*, 8981–9002.

Keppler, F., J. T. G. Hamilton, M. Brass, and T. Röckmann (2006), Methane emissions from terrestrial plants under aerobic conditions, *Nature*, *439*, 187–191, doi:10.1038/nature04420.

Lassey, K. R., E. A. Scheehle, and D. Kruger (2005), Towards reconciling national emission inventories for methane with the evolving global budget, *Environ. Sci.*, *2*, 193–204.

Melack, J. M., L. L. Hess, M. Gastil, B. R. Forsberg, S. K. Hamilton, I. B. T. Lima, and E. M. L. M. Novo (2004), Regionalization of methane emissions in the Amazon basin with microwave remote sensing, *Global Change Biol.*, *10*, 1–15.

Saueressig, G., P. Bergamaschi, F. N. Crowley, H. Fischer, and G. W. Harris (1995), Carbon kinetic isotope effect in the reaction of CH_4 with Cl atoms, *Geophys. Res. Lett.*, *22*, 1225–1228.

Taylor, K. E. (2001), Summarizing multiple aspects of model performance in a single diagram, *J. Geophys. Res.*, *106*, 7183–7192.

Walter, B. P., and M. Heimann (2000), A process-based, climate-sensitive model to derive methane emissions from natural wetlands: Application to five wetland sites, sensitivity to model parameters, and climate, *Global Biogeochem. Cycles*, *14*, 745–765.

I. Aben and M. Krol, Netherlands Institute for Space Research, Sorbonnelaan 2, NL-3584 CA Utrecht, Netherlands.

E. J. Dlugokencky, Earth System Research Laboratory, Boulder, CO 80305, USA.

C. Frankenberg, Institute of Environmental Physics, Heidelberg University, D-69120 Heidelberg, Germany.

S. Houweling, Institute for Marine and Atmospheric Research Utrecht, Princetonplein 5, NL-3584 CC Utrecht, Netherlands. (s.houweling@phys.uu.nl)

F. Keppler, Max Planck Institute for Nuclear Physics, D-69029 Heidelberg, Germany.

J. F. Meirink and T. Röckmann, Institute for Marine and Atmospheric Research Utrecht, Utrecht University, NL-3508 TA Utrecht, Netherlands.